Electronic states of the cap structure in the carbon nanotube

Ryo Tamura and Masaru Tsukada
Department of Physics, Graduate School of Science, University of Tokyo, Hongo 7-3-1, Bunkyo-ku, Tokyo 113, Japan
(Received 13 December 1994)

The cap of a carbon nanotube is characterized by six five-membered rings called disclinations. Its electronic structure is studied by the simple tight-binding models for a monolayer nanotube. The method of the development map is used to systematically define the atomistic structures of the cap. The topological feature of the bond network is determined by the configuration of the six five-membered rings. The effects of such topological features on electronic structure are elucidated by the model in which the hopping integrals and the site energies are taken to be common at every atom. Though there are neither disorder of the potential nor that of the coordination number, some localized states emerge around the cap. The wave function and the energy eigenvalue can be obtained analytically for simpler cases. These results show explicitly that the localized states are formed by an analytic continuation of the wave number from the real number space to the complex number space. Some of them are near the Fermi level and coexist with the extended states in the same energy. The effects of magnetic field parallel to the tube axis are also discussed.

I. INTRODUCTION

Many kinds of nanoscale materials made of curved layers of graphitic carbon have been reported recently and attracted much attention to their exotic structures. Typical examples are found in fullerenes,[1] graphitic nanotubes,[2] helically coiled tubes,[3,4] and related carbon structures.[5–7] It has been reported that nanotubes become semiconductors or metals according to their helicity and diameter.[8,9] The nanotubes have been treated as periodic infinite one-dimensional crystals in theoretical studies so far, but actual nanotubes have finite length. It is a natural idea that the edge of nanotubes takes the structure of a half fullerene. It means that the edge is closed without dangling bonds by introducing six five-membered rings in the honeycomb lattice. The five-membered ring is a topological defect which is a sort of disclination causing significant effects on the local electronic structure.[10] The configuration of the disclinations determines the topological structure of the bond network of the graphitic layer. In spite of the presence of the topological defect, the number of nearest-neighbor atoms is always 3 at each atom everywhere. We call the edge structure a "cap" and the nanotube with the cap a "capped nanotube" hereafter. The aim of the present paper is to investigate its influence upon the electronic state of the nanotube. There are many kinds of caps such as those with n-fold rotational symmetry with respect to the tube axis ($n=2,3,5,6$), and/or mirror symmetry, or without any symmetries. Among a variety of cap structures, we study in the present paper those with fivefold or sixfold rotational symmetry, since these are considered to be the prototypes of the cap. The cap is considered as a "surface" of the one-dimensional crystal of the nanotube and it is expected that there are "surface states," i.e., states localized at the cap. It will be shown in this paper that such localized states can occur even if there is no surface potential. Strangely enough, some of their discrete levels lie in the continuum of the density of states (DOS). In Ref. 10, we reported that a localized state emerges very near the Fermi level when a pair of a $4j$-membered ring ($j=$integer) and an odd-membered ring is introduced in the two-dimensional honeycomb lattice in some configurations. It is also caused by the topological disorder. This state decays as a power of the distance from the pair of disclinations and the exponent of the power nearly equals -1. We will report these features of the localization elsewhere. In sharp contrast to it, the localized states of the capped nanotubes discussed in the present work decay exponentially with distance from the cap. The localized states can be controlled by a magnetic field parallel to the tube axis, which will be discussed in connection with the axial rotational symmetry of the capped nanotubes in this paper. These localized states cause sharp peaks in the spectra which might affect various electronic phenomena. Especially the localized states near the Fermi level or in the gap might have much influence on transport phenomena.

II. MODEL FOR THE CALCULATION

A systematic way to construct cap structures of nanotubes is to draw the development map.[11] If the cap is made of six-membered and five-membered rings, it should include six five-membered rings. The way to make the development map of the cap is illustrated in Fig. 1. This is done by the following steps. (1) Cut a sector with the apex angle 60° from the perfect two-dimensional (2D) graphite lattice. (2) From this sector remove another sector whose sizes are parallel to the original sector. These removed sectors are shown by the shaded areas in Figs. 1(a) and 1(b). Here there are two cases: (i) any sides of the removed sector do not coincide with the sides of the original sector, or (ii) one side of the removed sector coincides with a side of the original sector. (3) For the case (i), connect the two corresponding dangling bonds direct-

 ©1995 The American Physical Society

ly which are formed by the removal of the inner sector. Then a semi-infinite belt of honeycomb lattice is formed as seen in Fig. 1(a). For the case (ii), a semi-infinite belt is already formed by the procedure (2) as seen in Fig. 1(b). In the case shown in Fig. 1(b), the belt includes only the zigzag line of the carbon atoms. (4) Connect six of five belts side by side with each other to form the six- or five-membered ring in the center. These correspond to Figs. 1(a) and 1(b), respectively. In this procedure the corresponding side atoms in the neighboring belts should be connected one by one. For the sake of explanation, the connection in the process (4) is illustrated by the dotted line, but there is no distinction between the original bonds (full line) and the new bonds (dotted line) in the actual system. We assume the same values of the hopping integrals between the atoms connected by the full lines or dotted lines and this value is represented by h ($h<0$) hereafter. A five-membered ring is always provided by the apex part of the removed sector. An additional five-membered ring appears at the central part, if the five semi-infinite belts are joined together as seen in Fig. 1(b).

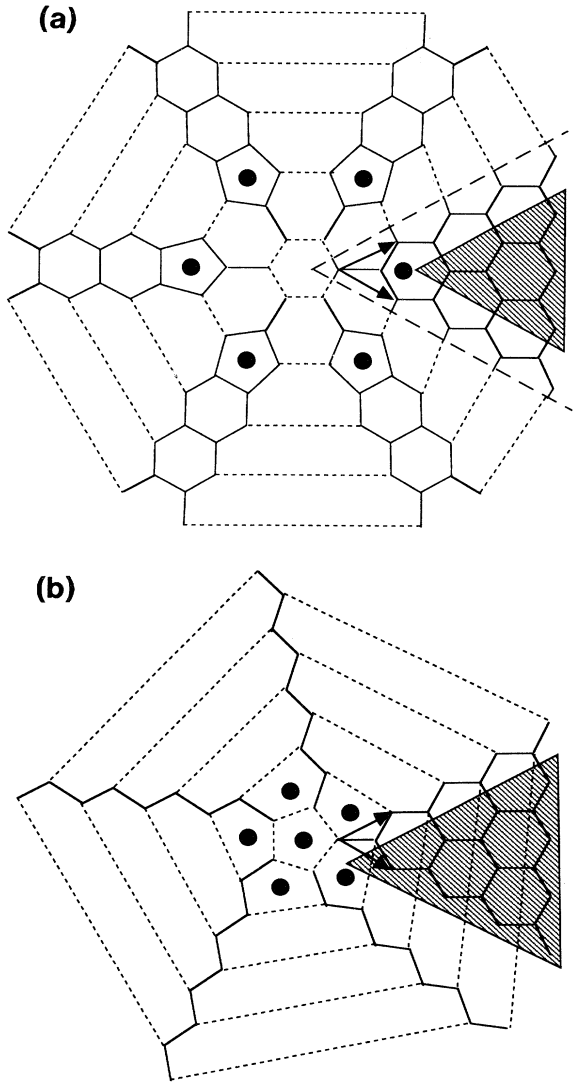

FIG. 1. Development maps of the capped nanotube. These are formed by connecting n belts side by side. $n=6$ in (a) and $n=5$ in (b). The black circles indicate positions of the six five-membered rings. Following the definition in the text, the belts in (a) are (1,1) and those in (b) are (1,0). The unit vectors used for the symbol (l,m) are represented by two arrows. The way to obtain the belt is illustrated in the right side of each figure; the original sector is shown by dashed lines in (a), and the shaded areas are the removed sectors. See text for details.

Once the connection between the atoms, i.e., the topological structure, is determined in this way, the Hamiltonian of the tight-binding model is defined as below. The carbon π orbital at site i will be indicated by $|i\rangle$, and for simplicity they are assumed to form an orthogonal normalized set. In the real system, the π orbital is mixed with the σ orbital, because the system is not on a flat plane. But this effect is ignored, since we are interested mainly in the topological feature of the capped nanotubes governed by the distributions of the five-membered rings; the effects caused by difference of the bond lengths and bond angles are ignored. The assumption is reasonable when the radius of curvature of the graphite layer is large. We choose the origin of energy as the common site energy $\langle i|H|i\rangle$, and assume the matrix elements of the Hamiltonian as

$$\langle i|H|j\rangle=\begin{cases}h & \text{if } i \text{ and } j \text{ are nearest neighbors}\\ 0 & \text{otherwise.}\end{cases}$$

Generally speaking the five or six belts connected to form the cap can be of different shape, respectively. For the sake of simplicity, however, we consider here only systems made of identical belts. Therefore the cap has axial symmetry with respect to the tube axis. To define the shape of the belt we use the symbol (l,m), which is the position vector of the inner sector apex relative to the original sector apex in the unit vectors of the 2D graphite shown in Fig. 1. The case (i) corresponds to $l\neq 0$ and $m\neq 0$ and the case (ii) corresponds to $l=0$ or $m=0$. The cap made of n ($=5$ or 6) (l,m) belts is identified by n-(l,m). The corresponding tube is specified by a pair of integers (nl,nm) in Ref. 8, so it is metallic when $n(l-m)$ is a multiple of 3 and semiconducting when $n(l-m)$ in not a multiple of 3. Following this definition the caps in Figs. 1(a) and 1(b) are represented by 6-(1,1) and 5-(1,0), respectively. The 5-(1,0) cap and the 5-(1,1) cap correspond to a half dodecahedron and a half C_{60}, respectively. The shapes of the 5-(1,1) cap and the 6-(1,1) cap are shown in Fig. 2.

Since the cap n-(l,m) belongs to the point group C_n, the electronic states are characterized by the characters of the irreducible representation $e^{i\beta_j}$, where $\beta_j=2\pi j/n$ with $j=0,1,\ldots,n-1$. We can block-diagonalize the original Hamiltonian into $H(\beta_j)$ with $j=0,1,\ldots,n-1$ describing the subsystem where only the atoms in the same belt are included. The hopping integral between the corresponding boundary atoms is multiplied by the phase factor $e^{i\beta_j}$ as illustrated by Fig. 3. If a magnetic field is applied along the tube axis, the phase should be continuously changed as

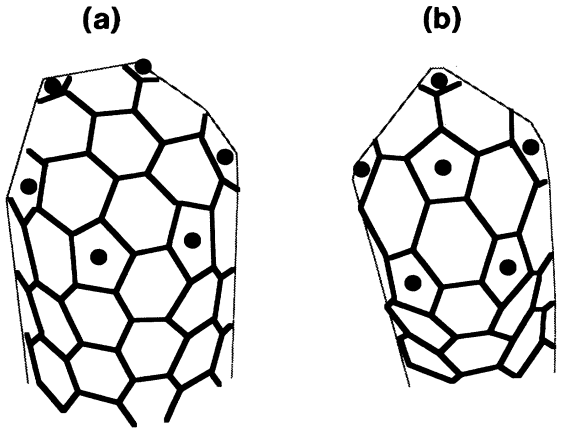

FIG. 2. The shape of the cap for (a) the 6-(1,1) cap and (b) the 5-(1,1) cap, where the positions of five-membered rings are shown by the filled circles.

$$\beta_j=\frac{2\pi j}{n}+\frac{2\pi\Phi}{n\Phi_0}\ , \tag{1}$$

where Φ is the value of the magnetic flux penetrating the n-membered ring at the top of the cap and Φ_0 is the value of the magnetic flux quantum. For simplicity, we assume that there is no magnetic flux penetrating the carbon plane except at the n-membered ring. In other words, we consider the Aharonov-Bohm effect. This assumption makes no significant difference from the actual case when the diameter of the tube is small. It is easily confirmed that the energy spectrum of $H(-\beta)$ coincides with that of $H(\beta)$, so the region of β is taken as $0\le\beta\le\pi$. The local density of states (LDOS) at the site j of the total system, $\rho_j(E)$, is obtained as

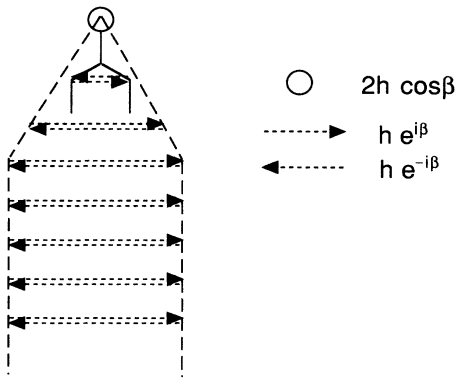

FIG. 3. The phase factor appearing in block-diagonalized Hamiltonian $H(\beta)$. Dashed lines represent the boundaries of the belt. h is the value of the hopping integrals of the inner bonds. For the bonds joining the boundary atoms with the corresponding atoms in the opposite boundary, which are introduced by the block diagonalization, the hopping integrals are multiplied by the phase factor $e^{\pm i\beta}$. They are shown by dotted arrows. Because the apex site is joined to itself by these bonds, it has the diagonal element $2h\cos\beta$ which is shown by the circle.

$$\rho_j(E)=\frac{1}{n}\sum_{i=1}^{n}\rho_j(E,\beta_i)\ , \tag{2}$$

where $\rho_j(E,\beta_i)$ is the local density of states at site j of the $H(\beta_i)$ system. When the magnetic field is absent, only the values of β 0, $\pm\frac{2}{5}\pi$, and $\pm\frac{4}{5}\pi$ for $n=5$ systems, and 0, $\pm\pi/3$, $\pm\frac{2}{3}\pi$, and π for $n=6$ systems are relevant. Therefore Eq. (2) becomes

$$\rho_j(E)=\tfrac{1}{5}\{\rho_j(E,0)+2\rho_j(E,\tfrac{2}{5}\pi)+2\rho_j(E,\tfrac{4}{5}\pi)\} \tag{3}$$

for $n=5$ and

$$\rho_j(E)=\tfrac{1}{6}\{\rho_j(E,0)+2\rho_j(E,\tfrac{1}{3}\pi)+2\rho_j(E,\tfrac{2}{3}\pi)+\rho_j(E,\pi)\} \tag{4}$$

for $n=6$. With the increase of the distance from the cap, the shape of the LDOS approaches that of the DOS of the corresponding tube without a cap. So the Fermi level E_F of the capped tube coincides with that of the tube without a cap, i.e., $E_F=0$.

III. ELECTRONIC STATES OF THE CAPPED NANOTUBE

For simpler systems such as n-(1,0) and n-(1,1), the edges of the continuum bands and the energy levels of the localized states are analytically determined, as will be discussed in Secs. III A and III B. The nondimensional parameter $\varepsilon=E/|h|=E/-h$ is used in these sections instead of E to simplify the notation. The energy spectrum of the Hamiltonian $H(\beta)$ is easily obtained by the recursion method for any values of β and (l,m),[12] as will be discussed in Sec. III C. The region of β is taken as $0\le\beta\le\pi$ without losing generality.

A. Green's function of n-(1,0) cap

In Fig. 4, the belt of (1,0) and the matrix elements of the block-diagonalized Hamiltonian $H(\beta)$ corresponding to the n-(1,0) cap are shown. The sites are numbered along the zigzag line of the (1,0) belt. The apex site is

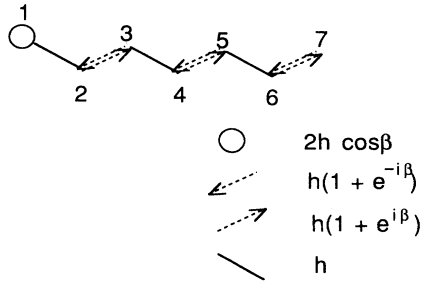

FIG. 4. The matrix elements of the block-diagonalized Hamiltonian corresponding to one-dimensional representation β for the case of the n-(1,0) cap. Sites are numbered along the zigzag line of the (1,0) belt. The two kinds of hopping integrals, h and $h(1+e^{\pm i\beta})$, appear alternately along this line and are represented by the solid lines and the dotted arrows, respectively. It has a diagonal element $2h\cos\beta$ only at the apex site which is shown by the circle.

numbered 1. The matrix element of $H(\beta)$ is given as

$$H(\beta)_{2j+1,2j}=H^*(\beta)_{2j,2j+1}=(1+e^{i\beta})h\equiv bh\ ,$$
$$H(\beta)_{2j,2j-1}=H(\beta)_{2j-1,2j}=h, \tag{5}$$
$$H(\beta)_{11}=2\cos\beta h\equiv Uh\quad (j\geq 1)\ .$$

The other matrix elements of $H(\beta)$ are zero. The nondimensional parameter $\varepsilon=E/|h|=E/-h$ is used instead of E to simplify the notation hereafter. The Green's function $G_{jj'}(E,\beta)\equiv[E-H(\beta)]^{-1}_{jj'}$ is derived as

$$\lim_{\delta\to+0}G_{j,j}(E-i\delta,\beta)=\frac{-\varepsilon}{|h|\mu}\left[1+\frac{r+s}{r-s}t^{\bar{j}-1}\right], \tag{6}$$

where

$$t=\frac{(\varepsilon^2-3-U+\mu)^2}{8+4U}\ , \tag{7}$$

$$\bar{j}=\begin{cases}\dfrac{j+1}{2} & \text{if } j=\text{odd}\\ \dfrac{j}{2} & \text{if } j=\text{even},\end{cases} \tag{8}$$

$$r=\begin{cases}\mu & \text{if } j=\text{odd}\\ (-\varepsilon-U)\mu & \text{if } j=\text{even},\end{cases} \tag{9}$$

and

$$s=\begin{cases}\varepsilon^2+2U\varepsilon+1+U\equiv f(\varepsilon) & \text{if } j=\text{odd}\\ (-\varepsilon-U)f(\varepsilon)+\dfrac{f(\varepsilon)^2-\mu^2}{2\varepsilon} & \text{if } j=\text{even}.\end{cases} \tag{10}$$

The range of the continuum of the spectrum is the same as that of the corresponding nanotube without the cap, i.e., $|\varepsilon_-|\leq|\varepsilon|\leq|\varepsilon_+|$, where

$$\varepsilon_\pm=2\cos\frac{\beta}{2}\pm 1\ . \tag{11}$$

When the energy is in the continuum of the spectrum $|\varepsilon_-|\leq|\varepsilon|\leq|\varepsilon_+|$, μ is a purely imaginary number:

$$\mu=\begin{cases}i\sqrt{(\varepsilon_+^2-\varepsilon^2)(\varepsilon^2-\varepsilon_-^2)} & \text{if } |\varepsilon_-|\leq\varepsilon\leq|\varepsilon_+|\\ -i\sqrt{(\varepsilon_+^2-\varepsilon^2)(\varepsilon^2-\varepsilon_-^2)} & \text{if } -|\varepsilon_-|\geq\varepsilon\geq-|\varepsilon_+|.\end{cases} \tag{12}$$

In this case, t is a complex number whose absolute value is 1. Half of its phase is the wave number of the corresponding extended state. On the other hand, when the energy is outside the continuum, μ is a real number:

$$\mu=\begin{cases}\sqrt{(\varepsilon^2-\varepsilon_+^2)(\varepsilon^2-\varepsilon_-^2)} & \text{if } |\varepsilon|\leq|\varepsilon_-|\\ -\sqrt{(\varepsilon^2-\varepsilon_+^2)(\varepsilon^2-\varepsilon_-^2)} & \text{if } |\varepsilon_+|\leq|\varepsilon|.\end{cases} \tag{13}$$

In this case, t is a real number less than 1. It corresponds to an analytic continuation of the wave number from the real number space to the complex number space. From this Green's function, the local density of states of the β band at the jth site, $\rho_j(E,\beta)$, is obtained as below:

$$\rho_j(E,\beta)=\frac{1}{\pi}\mathrm{Im}\lim_{\delta\to+0}G_{j,j}(E-i\delta,\beta)\ . \tag{14}$$

The first term of Eq. (6) turns out to be the density of states $\rho^0(E,\beta)$ of the β band of the corresponding nanotube without the cap given as below:

$$\rho^0(E,\beta)=\frac{1}{\pi}\frac{|\varepsilon|}{|h|\sqrt{(\varepsilon^2-\varepsilon_+^2)(\varepsilon_-^2-\varepsilon^2)}}\ . \tag{15}$$

The second term of Eq. (6) occurs from the interference between outgoing and incoming waves at the cap. Figure 5 shows the LDOS $\rho_1(E,\beta)$ for $\beta=0$, $\pi/3$, $\frac{2}{5}\pi$, $\frac{2}{3}\pi$, $\frac{4}{5}\pi$, and π, where the discrete levels discussed below are also shown by vertical lines. When $\beta=\pi$, $H(\beta)$ becomes the Hamiltonian of the set of independent molecules because $b=0$ so that there are no extended states and no continuous spectra in this case; the molecule of sites 1 and 2 has two discrete levels of $\varepsilon=U_\pm=1\pm\sqrt{2}$ given by Eq. (16), and the other molecules have those of $\varepsilon=\pm1$. The value of the Green's function is a real number outside the continuum region of the spectrum and has a pole when $r-s=0$. The pole corresponds to a localized state de-

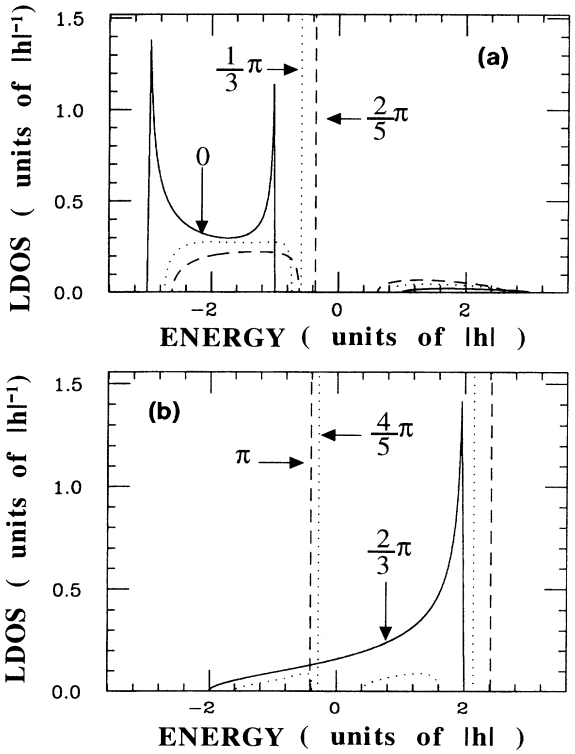

FIG. 5. The LDOS's of β bands at the apex site for the n-(1,0) cap. The solid line, the dotted line, and the dashed line in (a) [in (b)] correspond to $\beta=0(\beta=\frac{2}{3}\pi)$, $\beta=\pi/3(\frac{4}{5}\pi)$, and $\beta=\frac{2}{5}\pi$ (π), respectively. The unit of energy is the absolute value of the hopping integral, $|h|=-h$. The vertical lines show the discrete levels which are about $-0.59|h|$, $-0.41|h|$, $-0.36|h|$, $-0.29|h|$, $2.14|h|$, and $2.41|h|$. When $\beta=\pi$ there are no continua but only the discrete levels.

caying exponentially with distance from the cap as $|a_{2n-1}|^2$, $|a_{2n}|^2 \propto t^n$, where a_j is the amplitude of the eigenvector at site j, so the value of $\sqrt{t}$ is called the localization factor hereafter. The solution of ε for $r-s=0$ is

$$\varepsilon = -\frac{1}{2U}(U^2+U+2 \pm \sqrt{U^4-2U^3+U^2+4U+4}) \equiv U_{\pm} \tag{16}$$

on the condition that

$$|\varepsilon| \le |\varepsilon_-|, \quad f(\varepsilon) \ge 0 , \tag{17}$$

or

$$|\varepsilon| \ge |\varepsilon_+|, \quad f(\varepsilon) \le 0 , \tag{18}$$

where $f(\varepsilon)$ is defined by Eq. (10). The discrete energy level $\varepsilon = U_-$ appears in the region $|\varepsilon| \le |\varepsilon_-|$ for $0 \le \beta \le \pi$ and the level $\varepsilon = U_+$ appears in the region $|\varepsilon_+| \le \varepsilon$ for $\frac{2}{3}\pi \le \beta$. They are shown in Fig. 6 by the solid lines, where the continuum of the spectrum and its edges $\pm\varepsilon_{\pm}$ are shown by the shaded areas and the dashed lines, respectively. The localized state of $\varepsilon=0$ and $\beta=\frac{1}{2}\pi$ has a unique feature; amplitudes of its wave function are zero at even-number sites so that the pole at $\varepsilon=0$ appears only at odd-number sites.

The wave function with its energy at the band edge has an infinitely long wavelength, so it cannot satisfy the boundary condition at the cap except in special cases. The states at the band edge which can exist only in special cases are called "critical states" hereafter. The critical states of the n-(1,0) cap appear when $|\varepsilon| = |\varepsilon_{\pm}|$ and $f(\varepsilon)=0$ which is the particular case of the condition (17) or (18). The critical state of $\beta=0$, $\varepsilon=-3$ is the self-evident solution of the Schrödinger equation; it has the same amplitude at every site. The other critical states of $(\beta,\varepsilon)=(0,-1)$, $(\frac{2}{3}\pi,0)$, and $(\frac{2}{3}\pi,2)$ appear as the limit of the cap states as can be seen in Fig. 6. This can be confirmed also by the localization factor $\sqrt{t}$ shown in Fig. 7 by the solid line and dotted line for U_- and U_+, respectively; as the discrete level approaches the band edges, the localization factor $\sqrt{t}$ increases to unity, i.e., the localized state approaches the critical state. At the band edges with the critical state, the LDOS $\rho_j(E,\beta)$ behaves in the same way as $\rho^0(E,\beta)$ shown in Eq. (15). That is to say, when $(\beta,\varepsilon)=(0,-1)$, $(0,-3)$, and $(\frac{2}{3}\pi,2)$ it has inverse square-root divergence, and when $\beta=\frac{2}{3}\pi$, $\varepsilon=0$ it has a finite value $1/2\pi$ as seen in Fig. 5.

But at the other band edges without the critical state, i.e., when $r=0$, $s\neq 0$, the LDOS continuously goes to zero in contrast to $\rho^0(E,\beta)$. These behaviors of $\rho_j(E,\beta)$ at $\varepsilon=\pm\varepsilon_{\pm}$ can be confirmed by the expansion of $G_{j,j}(E,\beta)$ in terms of r/s or s/r. The total LDOS's at the site 1 in the case of no magnetic field for $n=6$ and 5 are shown by solid line and the dot-dashed line in Fig. 8, where the discrete levels are also shown by the vertical lines. It shows that the 5-(1,0) cap is a semiconductor and the 6-(1,0) cap is a metal. The derivative is discontinuous at the edge of the β band without the critical state. The discrete levels of U_- at $\beta=\pi/3$ and π enter in the continuum spectral range of the 6-(1,0) cap, and that of U_+ at $\beta=\frac{4}{5}\pi$ (at $\beta=\pi$) enters in the continuum spectral range of the 5-(1,0) cap [6-(1,0) cap]. Though the discrete levels are outside the continuum of the $H(\beta)$ which they belong to, they can enter in the continuum of the other $H(\beta')$ $(\beta' \neq \beta)$. Even if the localized state and the extend state coexist at the same energy, they are not mixed because they have different rotational symmetries. The presence of the localized states buried in the continuum of the extended states is often observed in general capped tubes as will be seen in the following sections. Though the n-(1,0) cap may be unrealistic because the five-membered rings are fused, it has some common gen-

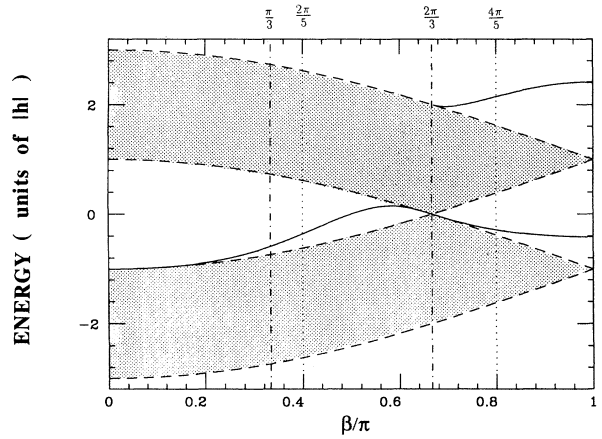

FIG. 6. The discrete energy levels of the localized states vs β for the n-(1,0) cap. They are shown by solid lines. The unit of energy is the same as in Fig. 5. The shaded area shows the region of the continuum spectra whose edges are represented by dashed lines. The vertical dot-dashed lines and dotted lines indicate $\beta=(\pi/3)j$ and $\frac{2}{5}\pi j (j=1,2)$, respectively.

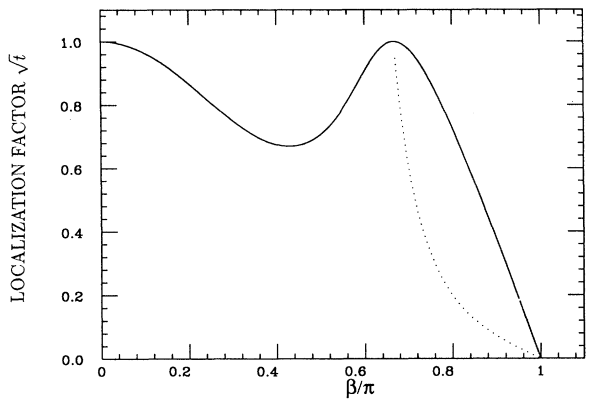

FIG. 7. The localization factor $\sqrt{t}$ vs β for the n-(1,0) cap where t is defined in Sec. III A. The absolute value of the wave function of the localized state is proportional to $\sqrt{t}^j$ where j represents the distance from the cap. The solid line and the dotted line correspond to the discrete levels $E=U_-$ and $E=U_+$, respectively.

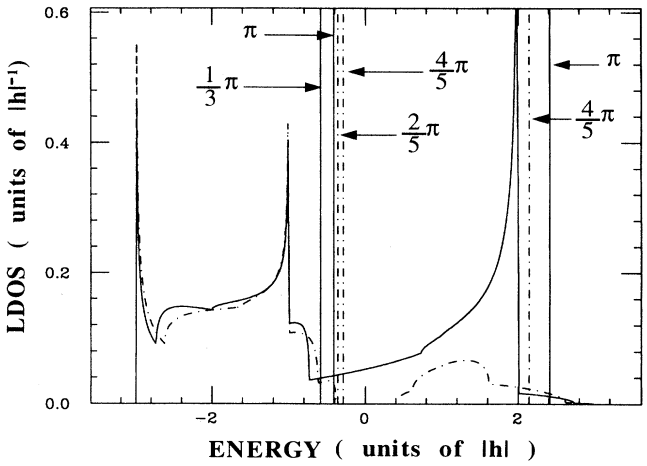

FIG. 8. Local density of states at the apex site in the n-(1,0) cap. The unit of energy is the same as that of Fig. 5. The solid line and the dot-dashed line correspond to $n=6$ and 5, respectively. The vertical lines indicate the discrete energy levels. The values of β that each discrete level belongs to are also shown.

eral features with certain kinds of caps as will be seen in Sec. III C.

B. Localized states of the n-(1,1) cap

The amplitudes of the wave function of $H(\beta)$, i.e., $\{p_j\}$ and $\{q_j\}$ shown in Fig. 9, whose energy is ε, are given by

$$\begin{aligned} p_{2j+1} &= cw_1^{j-1} , \\ p_{2j+2} &= w_1^j , \\ q_{2j+1} &= \frac{w_1^j}{w_2} , \\ q_{2j+2} &= \frac{cw_1^j}{w_2} \quad (j \geq 1) , \end{aligned} \tag{19}$$

where complex numbers w_1, w_2, and c have to satisfy the following two equations:[13]

$$\varepsilon = \pm\sqrt{(1+w_1+w_2)(1+w_1^{-1}+w_2^{-1})} , \tag{20}$$

$$c = \frac{1+w_1+w_2}{-\varepsilon} = \frac{-\varepsilon}{1+w_1^{-1}+w_2^{-1}} . \tag{21}$$

From the boundary condition for the circumferential direction of the nanotube expressed by $w_2^2/w_1 = e^{i\beta}$,[8,9] w_1 and w_2 can be written as

$$\begin{aligned} w_1 &= x^2 e^{i2\alpha} , \\ w_2 &= x e^{i(\alpha+\beta/2)} \quad (0 < x \leq 1, \ -\pi < \alpha \leq \pi) . \end{aligned} \tag{22}$$

So this wave function is represented by $\phi(x,\alpha)$ hereafter. In the case of the perfect nanotube without cap, x must

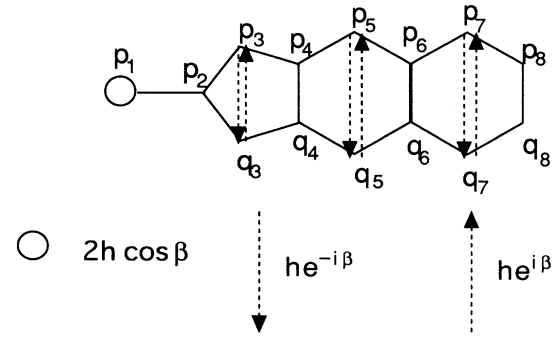

FIG. 9. The matrix elements and the wave function of the block-diagonalized Hamiltonian corresponding to the one-dimensional representation β for the case of the n-(1,1) cap. The amplitudes of the wave function are represented by p_j and q_j where the integer j shows the distance from the apex site. The two kinds of hopping integrals h and $he^{\pm i\beta}$ are represented by the solid lines and the dotted line arrows, respectively. It has a diagonal element $2h\cos\beta$ only at the apex site, which is shown by the circle.

be 1 and 2α is the wave number. In contrast to it, it is shown in Table I that the n-(1,1) capped tube can have states of $x \leq 1$ which exponentially decay with distance from the cap. These states are obtained by an analytic continuation of the wave number from the real number space to the complex number space. The equations to determine x and ε in Table I come from the Schrödinger equation $-\varepsilon p_2 = p_1 + p_3 + q_3$ and their solutions can be gained easily by numerical calculations. The amplitudes at sites 1 and 2 are taken as $p_1 = p_2 = 0$ in (3) and $p_1 = -1/(\varepsilon + U)$, $p_2 = 1$ in the other cases.

At least one of the four conditions (i), (ii), (iii), and (iv) shown below has to be satisfied, because the imaginary part of ε^2 must be zero. The satisfied condition(s) is (are) also listed in Table I. The four conditions are

$$\text{(i)} \quad \left[x + \frac{1}{x}\right]\cos\alpha + \cos\frac{\beta}{2} = 0 , \tag{23}$$

$$\text{(ii)} \quad \alpha = 0 , \tag{24}$$

$$\text{(iii)} \quad \alpha = \pi , \tag{25}$$

and

$$\text{(iv)} \quad x = 1 . \tag{26}$$

The condition (iv) corresponds to the extended states which form the bands of the continuum shown by the shaded areas in Fig. 10. The region of the continuum spectrum is

$$\sin\frac{\beta}{2} \leq |\varepsilon| \leq \sqrt{5+4\cos(\beta/2)} . \tag{27}$$

It coincides with that of the corresponding nanotube without the cap. Table I(a) shows the case when the localized states and the critical states appear for only a certain value of β. The state (1) has the same amplitudes at every site and is not a localized state but a critical state causing divergence at the band edge of the LDOS, as will

be seen later. The localized state (2) is symmetric about the mirror plane of the (1,1) sector, i.e., $p_i = q_i$ ($i \geq 3$). So we call it the symmetric localized state hereafter. It seems strange that the symmetric localized state lies in the continuum spectrum of the $\beta=0$ band. But it is understandable when one notices the following. The bands of β can be divided into two subbands with a definite symmetry, i.e., symmetric or antisymmetric about the mirror plane only when $\beta=0$ or π. In the case of $\beta=\pi$, the continuous spectrum of the symmetric subband and that of the antisymmetric subband coincide with each other. But in the case of $\beta=0$ they are different from each other; $-3 \leq \varepsilon \leq 1$ for the symmetric subband and $-1 \leq \varepsilon \leq 3$ for the antisymmetric subband. The symmetric localized state of $\beta=0$ lies outside the continuous spectrum of the symmetric subband but buried within that of the antisymmetric subband. When $\beta \neq 0$, the symmetric localized state changes into the resonant state. The smaller the $|\beta|$ value, the sharper is the resonant peak in the spectra. However, it is rapidly widened and the peak intensity is reduced with increase of β, as seen in Fig. 11. This indicates that this localized state is sensitive to the magnetic field; it changes into a resonant state discontinuously. That the symmetric localized state appears when $l=m$, i.e., when the (l,m) belt has a mirror plane, is confirmed also for the other n-(l,m) caps by the recursion method. Its energy is about $2.43|h|$ when $l=m=2$ and about $2.73|h|$ where $l=m=3$. The state (3) is a critical state at the band edge $\varepsilon=-1$ whose amplitudes are zero at site 1 and $2j$ sites. So it causes inverse square-root divergence at $\varepsilon=-1$ in the LDOS only at $(2j+1)$th sites ($j \geq 1$).

TABLE I. The equations to determine the localization factor x and the energy ε of the localized states and the critical states in the n-(1,1) capped tube. The condition for $\mathrm{Im}(\varepsilon^2)=0$ is also shown. The equations are listed for various values (ranges) of the phase β and the energy ε. See the text for the definition of $\phi(x,\alpha)$ and the physical meaning of β, x, α, and $\mathrm{Im}(\varepsilon^2)=0$. (a) corresponds to the case when the localized states and the critical states appear for only a certain value of β and (b) to the case when they appear for a finite range of β.

(a)

	(1)	(2)	(3)
β	0	0	π
ε	-3	$-1+x+\frac{1}{x} \simeq 1.383$	-1
Wave function	$\phi(1,0)$	$\phi(x,\pi)$	$\phi\left[1,\frac{\pi}{2}\right]-\phi\left[1,-\frac{\pi}{2}\right]$
Equation to determine x and ε		$x^3+x^2+x-1=0$ ($x \simeq 0.5437$)	
Condition(s) satisfied for $\mathrm{Im}(\varepsilon^2)=0$	(ii),(iv)	(iii)	(i),(iv)

(b)

	(4)	(5)
Range of β $\beta_1 \leq \beta \leq \beta_2$	$\beta_1=0, \beta_2 \simeq 0.64\pi$	$\beta_1 \simeq 0.73\pi, \beta_2=\pi$
Range of ε	$\lvert\varepsilon\rvert \leq \sin\frac{\beta}{2}$	$\lvert\varepsilon\rvert \geq \sqrt{5+4\cos(\beta/2)}$
Wave function	$z_1\phi(x,\alpha)+z_2\phi(x,-\alpha)$	$z_-\phi(x_-,0)+z_+\phi(x_+,\pi)$
Equation to determine x and ε	$-\varepsilon+\frac{1}{\varepsilon+U}-z_1d_+-z_2d_-$ $-xe^{-i\beta/2}(z_1e^{i\alpha}+z_2e^{-i\alpha})=0$ where $d_\pm=\frac{1+x^2e^{\pm 2i\alpha}+xe^{i(\pm\alpha+\beta/2)}}{-\varepsilon}$, $z_1=1-z_2=\frac{1}{2}-\frac{-i\varepsilon e^{i\beta/2}+\sin(\beta/2)}{2(x-1/x)\sin\alpha}$, $\cos\alpha=-\left[\frac{5-\varepsilon^2-\sqrt{(5-\varepsilon^2)^2-16\cos^2(\beta/2)}}{8}\right]^{1/2}$, and $x=\frac{1}{2}\left\{-\frac{\cos(\beta/2)}{\cos\alpha}-\left[\frac{\cos^2(\beta/2)}{\cos^2\alpha}-4\right]^{1/2}\right\}$.	$-\varepsilon+\frac{1}{\varepsilon+U}-z_+c_+$ $-z_-c_--(z_-x_--z_+x_+)e^{-i\beta/2}=0$ where $c_\pm=\frac{1+x_\pm^2\mp x_\pm e^{i\beta/2}}{-\varepsilon}$, $z_\pm=\frac{1}{2}\pm\frac{i\sin(\beta/2)+\varepsilon e^{i\beta/2}}{2\sqrt{\varepsilon^2-\sin^2(\beta/2)}}$, and $x_\pm+\frac{1}{x_\pm}=\sqrt{\varepsilon^2-\sin^2(\beta/2)}\pm\cos\frac{\beta}{2}$.
Condition(s) satisfied for $\mathrm{Im}(\varepsilon^2)=0$	(i)	(ii), (iii)

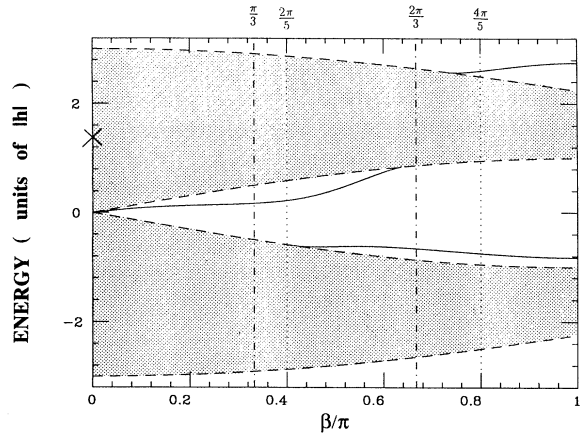

FIG. 10. The discrete energy levels of the localized states vs β for the n-(1,1) cap. They are shown by solid lines. The unit of energy is the same as in Fig. 5. The vertical lines, the shaded area, and the dashed lines have the same meanings as those of Fig. 6. The energy level of the symmetric localized state which can exist only when $\beta=0$ is shown by a cross.

Table I(b) shows another type of localized states which exist in a finite range of β unlike the symmetric localized state that exists only when $\beta=0$. Their discrete levels are shown in Fig. 10 by solid lines. There are two branches of discrete levels of the type (4). One has a positive energy and the other has a negative energy. Another branch of the discrete level of type (5) lies above the upper continuous band. As in the case of the n-(1,0) cap, critical states occur when these branches coincide with the band edges, i.e., when $(\beta,\varepsilon)\sim(0.41\pi,-0.61)$, $(0.64\pi,0.84)$, and $(0.73\pi,2.57)$ and $(\beta,\varepsilon)=(0,0)$. The behavior at the band edges of the LDOS of the β band is determined by whether there is a critical state or not just in the same way as in the case of the n-(1,0) cap. In Fig. 12, the solid lines and the dotted lines show x^2 corresponding to the types (4) and (5), respectively. The value of x^2 is called

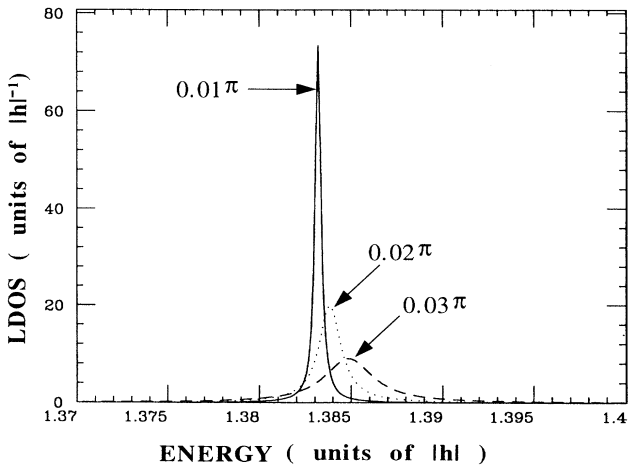

FIG. 11. LDOS's of the n-(1,1) cap near $E=1.383|h|$ for $\beta=0.01\pi$, 0.02π, and 0.03π. The sharp resonant peak becomes dull as β increases.

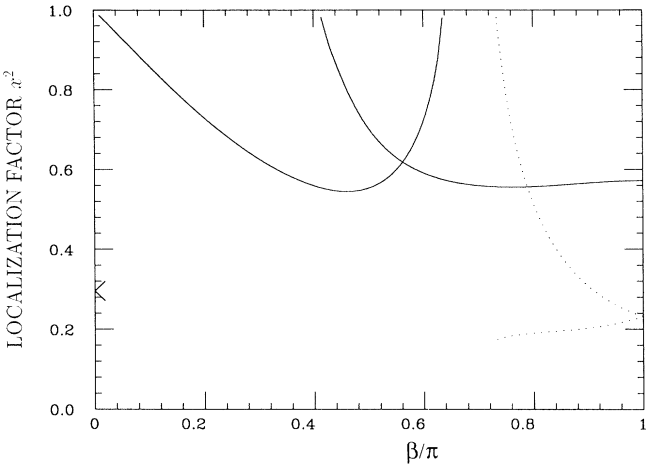

FIG. 12. The localization factor x^2 vs β for the n-(1,1) cap where x is defined in Sec. III B. The absolute value of the wave function of the localized state is proportional to x^{2j} where j represents distance from the cap. The solid line and the dotted line correspond to the discrete levels in the gap and those above the upper continuous band, respectively. The latter localized states are a superposition of the two degenerate states having different values of x^2 both of which are shown in this figure.

the localization factor hereafter because it determines the exponent of the localization. The type (5) has two different values of x^2, x_-^2 and x_+^2, of which x_-^2 should be taken as the localization factor because $x_- \geq x_+$. The localization factor behaves also in the same way as that of the n-(1,0) cap. That is to say, as the discrete level leaves the band edge, the localization factor becomes smaller, i.e., it decays more rapidly. This character is similar to that of impurity levels in the gap of semiconductors.

In Fig. 13, the LDOS's of the β bands at the site belonging to the n-membered ring are shown for $\beta=0$, $\pi/3$, $\frac{2}{5}\pi$, $\frac{2}{3}\pi$, $\frac{4}{5}\pi$, and π. They are calculated numerically with Haydock's recursion method explained in the next section. The discrete levels obtained in this section are also shown by the vertical lines in Fig. 13. The LDOS of $\beta=0$ is divergent at $\varepsilon=-3$ because of the critical state [(1) in Table I]. The LDOS's of $\beta=\frac{2}{5}\pi$ and $\frac{2}{3}\pi$ have sharp peaks near the lower and the upper gap edges, respectively. They are precursor states of the localized states of type (4) as is understood by Fig. 10. The latter resonant peak becomes widened and lowered as β increases as is shown by the peak near $\varepsilon=1.5$ when $\beta=\frac{4}{5}\pi$ and near $\varepsilon=1.8$ when $\beta=\pi$. There are also small peaks near $\varepsilon=1.6$ for $\beta=\pi/3$ and $\frac{2}{5}\pi$ and near $\varepsilon=2.4$ for $\beta=\frac{2}{3}\pi$. They are resonant with the symmetric localized state of $\beta=0$, $\alpha=\pi$, $\varepsilon=1.383$ as well as with the discrete level above the upper continuous band. In this way, type (2) and type (5) shown in Table I are connected continuously by resonant states. The LDOS's at the apex site are shown in Fig. 14 for $n=5$ and 6 by the solid line and by the dot-dashed line, respectively, in the case of no magnetic field. Both of them have no gap, i.e., they are metallic, since the band of $\beta=0$ has no gap. The discrete levels are shown by the vertical lines. The total continuous spec-

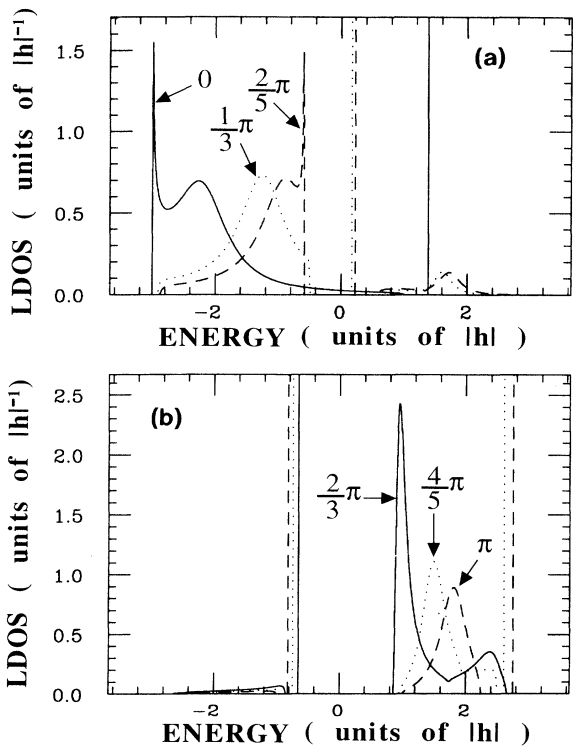

FIG. 13. The LDOS's of β bands at the apex site for the n-(1,1) cap. The correspondence between the types of lines and β is the same as in Fig. 5. The unit of energy is the same as in Fig. 5.

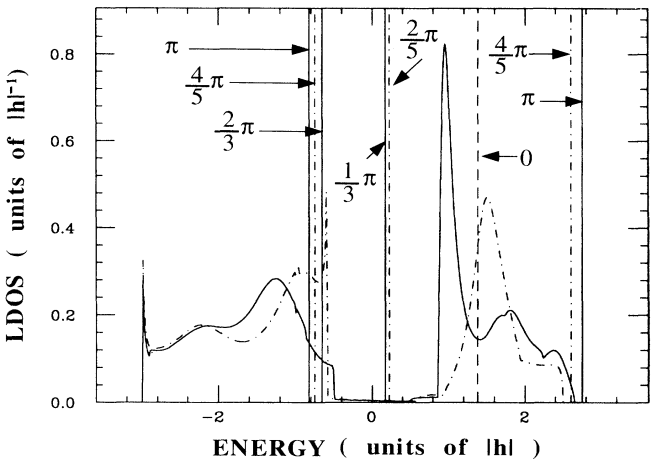

FIG. 14. Local density of states at the apex site in n-(1,1) cap. The unit of energy is the same as that of Fig. 5. The solid line and the dot-dashed line correspond to $n=6$ and 5, respectively. The vertical lines indicate the discrete energy levels. The dashed vertical line indicates the discrete level appearing in both the 5-(1,1) cap and 6-(1,1) cap. The values of β that each discrete level belongs to are also shown. The discrete energy levels are about $-0.82|h|$, $-0.75|h|$, $-0.66|h|$, $0.17|h|$, $0.22|h|$, $1.38|h|$, $2.60|h|$, and $2.75|h|$.

trum of the n-(1,1) cap has the energy range $-3\leq\varepsilon\leq 3$ in which all the discrete levels appear. But the LDOS's in Fig. 14 are zero near $\varepsilon=3$ since the LDOS's at a site on the mirror plane such as the apex site do not include the antisymmetric subband of $\beta=0$ whose continuous spectrum is $-1\leq\varepsilon\leq 3$. As in the case of the n-(1,0) cap, localized states and extended states with different symmetries exist at the same energy. The symmetric localized state of $\beta=0$ appears in both the 5-(1,1) cap and the 6-(1,1) cap.

C. General capped nanotubes

In the case of n-(l,m) caps where $l>1$ and/or $m>1$, it is difficult to obtain the analytical solution of their Green's function or localized states. But it is easy to calculate numerically the Green's function by Haydock's recursion method. We give a brief summary of Haydock's recursion method relevant to the present system.[12]

The index 0 is assigned to the site where we want to obtain the LDOS, $\rho_0(E)$. Then $G_{00}(E)$ is given by the recursion formula

$$G_{00}(E)=\frac{1}{[E-a_1-b_1g_1(E)]}\ , \tag{28}$$

$$g_1(E)=\frac{1}{[E-a_2-b_2g_2(E)]}\ ,$$

$$\vdots \qquad\qquad \vdots$$

$$g_{j-1}(E)=\frac{1}{[E-a_j-b_jg_j(E)]}\ , \tag{29}$$

where $a_j=\{j|H|j\}/\{j|j\}$ and $b_{j-1}=\{j|j\}/\{j-1|j-1\}$ with $|j\}$ defined by the standard recursion formula. Then $\rho_0(E)$ is obtained from the Green's function $G_{00}(E)$ by Eq. (14). The above procedure can be continued to any desired values of j. When a_j and b_j converge to an essentially constant value after N steps of the above process, we can terminate this process with Eq. (30):

$$g_{N-1}(E)=\frac{(E-a_N)}{2b_N}\left\{1-\left[1-\frac{4b_N}{(E-a_N)^2}\right]^{1/2}\right\}\ . \tag{30}$$

If the block-diagonalized Hamiltonian $H(\beta)$ is substituted for the total Hamiltonian H in the above procedure, the LDOS of the β band is obtained instead of the total LDOS. But it sometimes occurs that a_{2j} and b_{2j} converge to a different value from a_{2j-1} or b_{2j-1}, respectively, as

$$\begin{aligned}&\lim_{j\to\infty}a_{2j-1}=a_o\ ,\\ &\lim_{j\to\infty}a_{2j}=a_e\ ,\\ &\lim_{j\to\infty}b_{2j-1}=b_o\ ,\\ &\lim_{j\to\infty}a_{2j}=b_e\ .\end{aligned} \tag{31}$$

One example is the case of the n-(1,0) cap. The corresponding $H(\beta)$ has already a tridiagonal form as discussed in Sec. III A. Therefore if site 0 is taken as site 1,

that is, the apex site of the (1,0) belt, $\{a_j\}$ and $\{b_j\}$ are explicitly obtained:

$$a_1=2\cos\beta h\ ,$$
$$a_j=0,\quad j\geq 2\ , \tag{32}$$

$$b_j=\begin{cases}h^2, & j=\text{odd}\\ (2+2\cos\beta)h^2, & j=\text{even.}\end{cases} \tag{33}$$

In such a case, another termination should be used:

$$g_e(E)=\frac{1}{E-a_o-b_o g_o(E)}\ , \tag{34}$$

$$g_o(E)=\frac{1}{E-a_e-b_e g_e(E)}\ , \tag{35}$$

where

$$\lim_{j\to\infty} g_{2j-1}(E)\equiv g_o(E)\ , \tag{36}$$

$$\lim_{j\to\infty} g_{2j}(E)\equiv g_e(E)\ . \tag{37}$$

Solving this simultaneous equation,

$$g_e(E)=\frac{1}{2b_e(E-a_o)}\{(E-a_o)(E-a_e)-b_o+b_e\pm\sqrt{(E-E_1^+)(E-E_1^-)(E-E_2^+)(E-E_2^-)}\}\ , \tag{38}$$

where

$$E_1^{\pm}=\frac{1}{2}\{a_e+a_o\pm[(a_o-a_e)^2+4(\sqrt{b_e}+\sqrt{b_o})^2]^{1/2}\}\ , \tag{39}$$

$$E_2^{\pm}=\frac{1}{2}\{a_e+a_0\pm[(a_o-a_e)^2+4(\sqrt{b_e}-\sqrt{b_o})^2]^{1/2}\}\ , \tag{40}$$

$$E_1^+>E_2^+\geq E_2^-\geq E_1^-\ . \tag{41}$$

The equality in the relation (41) is satisfied only when $a_o=a_e$ and $b_e=b_o$. In practice, a_{2M+1}, a_{2M}, b_{2M+1}, and b_{2M} are substituted for a_o, a_e, b_o, and b_e, respectively, where $2M+1$ is the number of steps needed for enough convergence of a_j and b_j. Then $g_e(E)$ obtained by this substitution is used instead of $g_{2M}(E)$.

When $E_1^+\leq E\leq E_2^+$, $E_1^-\leq E\leq E_2^-$, which corresponds to the continuous spectrum, $g_e(E)$ has a finite imaginary part which comes from the square root in Eq. (38) and the LDOS at a particular site 0 is obtained from the imaginary part of the Green's function. Outside the continuous spectrum, $g_e(E)$ becomes a real number and the discrete level can be found from the pole of the Green's function. The sign of the root in Eq. (38) should be taken as + when $E_2^-\leq E\leq E_2^+$ and − when $E\geq E_1^+$ or $E_1^-\geq E$. In this paper, we take the termination step $2M+1$ as 81–101.

The localized states and the band edges of the n-(l,m) cap, $E_1^{\pm}$ and $E_2^{\pm}$, obtained by the recursion method are classified according to $l-m$. They are similar to those of the n-(1,0) cap when $l-m$ is not a multiple of 3, and similar to those of the n-(1,1) cap when $l-m$ is a multiple of 3. These examples are shown in Fig. 15. Figures 15(a) and 15(b) show the discrete levels by the cross marks and the band edges by the dashed lines for $(l,m)=(4,1)$ and (2,1), respectively. They are calculated for 61 values of β, $\beta=\pi j/60$ ($j=0$–60). The continuous spectrum is shown by the shaded area. The gap is closed at $\beta=0$ when $l-m$ is a multiple of 3, and at $\beta=\frac{2}{3}\pi$ when $l-m$ is not a multiple of 3. But there are some differences compared to the case of $(l,m)=(1,0)$ or (1,1). As l and m become larger, $|E_1^{\pm}|$ and $|E_2^{\pm}|$ approach zero and $3|h|$, respectively, i.e., the energy region outside the continuous band, $-3|h|\leq E\leq E_1^-$, $E_2^-\leq E\leq E_2^+$, $E_1^+\leq E\leq 3|h|$, becomes smaller. This is consistent with the semiconductor nanotube whose gap becomes smaller

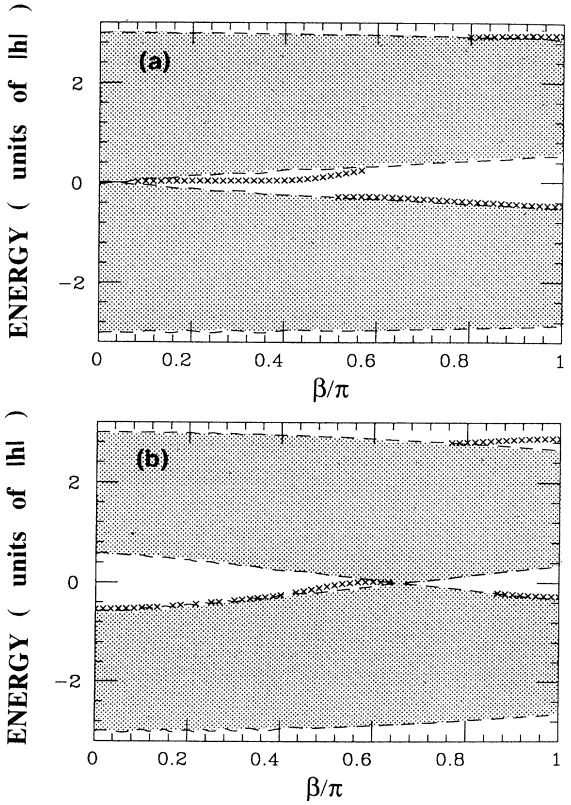

FIG. 15. The discrete energy levels of the localized states vs β for (a) n-(4,1) cap and (b) n-(2,1) cap. They are calculated for 61 values of β, $\beta=(j/60)\pi$ ($j=0$–60), and are shown by the crosses. The unit of energy is the same as in Fig. 5. The shaded area and the dashed lines have the same meanings as those of Fig. 6.

as its diameter becomes larger. As a result, the discrete levels approach the band edges and the region of β where the discrete level exists becomes gradually narrower. The LDOS's of the β band, $\rho_0(\beta,E)$ ($\beta=0$, $\frac{1}{3}\pi$, $\frac{2}{5}\pi$, $\frac{2}{3}\pi$, $\frac{4}{5}\pi$, and π), obtained by the recursion method are shown in Fig. 16 for $(l,m)=(4,1)$ and in Fig. 17 for $(l,m)=(2,1)$. The site 0 is taken to be the apex site. For the case of $(l,m)=(2,1)$, the discrete level in the gap does not coincide with the lower gap edge at $\beta=0$ unlike the case of $(l,m)=(1,0)$, but is quite close by it at $\beta=\frac{1}{3}\pi$ and at $\beta=\frac{2}{5}\pi$ as seen in Fig. 15, so that the LDOS of $\beta=0$ is not divergent at the lower gap edge unlike the case of the n-(1,0) cap, but the LDOS's of $\beta=\frac{1}{3}\pi$ and $\frac{2}{5}\pi$ have sharp resonant peaks there as seen in Fig. 17. The LDOS of $\beta=0$ ($\beta=\frac{2}{3}\pi$) has no gap and takes a finite value at the Fermi level when $l-m$ is a multiple of 3 (when $l-m$ is not a multiple of 3). Though the LDOS of the band $\beta=0$ in Fig. 16 has a very small value near the Fermi level, a large enough value of the LDOS appears there at a site far from the apex site. In this way, when $l-m$ is a multiple of 3 the amplitude of the wave function for $\beta=0$ around the Fermi level is smaller at the top of the cap than that at sites far from it. As in the cases of the n-(1,0) and the n-(1,1) cap, discrete levels exist in the total continuous band. As l and m increase, i.e., as the distances between five-membered rings increase, the LDOS shows more oscillations caused by interference of the waves from the different five-membered rings. In addition to

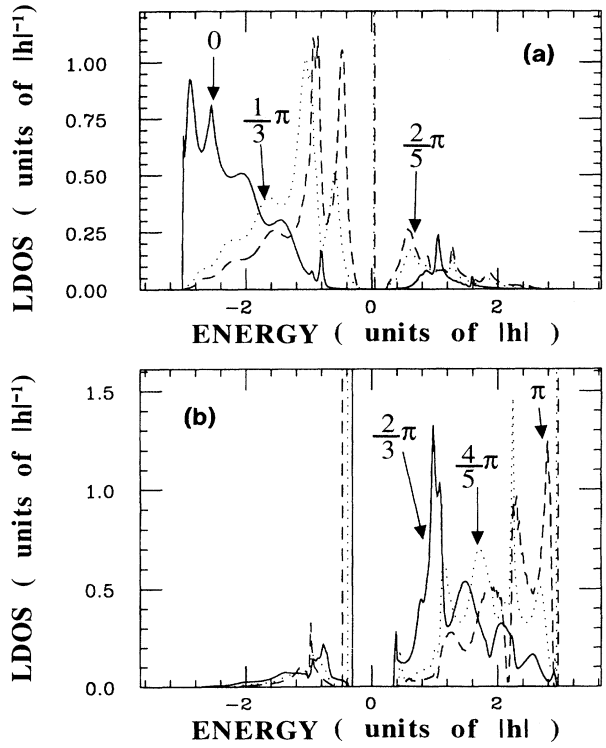

FIG. 16. The LDOS's of β bands at the apex site for the n-(4,1) cap. The correspondence between the types of lines and β is the same as in Fig. 5. The unit of energy is the same as in Fig. 5.

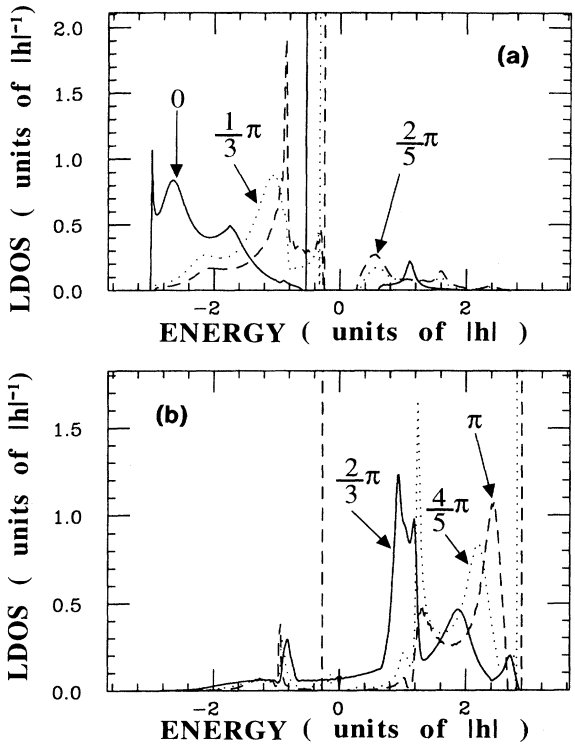

FIG. 17. The LDOS's of β bands at the apex site for the n-(2,1) cap. The correspondence between the types of lines and β is the same as in Fig. 5. The unit of energy is the same as in Fig. 5.

that, sharp peaks emerge showing the Van Hove singularity, e.g., the peak for $(l,m)=(2,1)$, $\beta=\frac{2}{5}\pi$, $E\simeq-0.9|h|$.

IV. SUMMARY AND DISCUSSION

In this paper, the important effect of the cap structure of the nanotube is demonstrated. It causes localized states decaying exponentially with distance from the cap. The mechanism of the appearance of the localized states is neither due to the local potential nor due to the change of the coordination number, since the model assumes a constant site energy and a constant hopping integral everywhere and the coordination number at every site is 3. Therefore the localization of the state is due to the topological disorder caused by the assembly of the six five-membered rings. The localized states are caused by an analytic continuation of the wave number from the real number space to the complex number space. This point is demonstrated most clearly in the simpler cases of the n-(1,0) and n-(1,1) caps; the imaginary part of the wave number appears as a localization factor whose analytic form is given without ambiguity and shows the localization feature. Though it becomes difficult to show such a clear result about general caps, we believe that the essence of the appearance of the localized states is the same as that of the simple special cases. Interestingly, some of the localized states coexist with extended states at the same energy without being mixed with each other because they have different symmetries. If there are per-

turbations that mix the states with the different symmetries, such as phonons, bond alteration, electromagnetic field, and so on, the discrete level in the continuum will be mixed with the extended states and become a sharp resonant state which can carry electric current. The appearance of such a sharp resonant state close to the Fermi level might induce remarkable properties of the cap of nanotubes from the viewpoint of applications. For example, excellently coherent electron emission can be expected from the cap of the nanotube, which is quite ideal for a scanning tunneling microscopy (STM) tip and electron source materials.

Aside from the fact that the gap is generated by the magnetic field,[14] it is significant that the localized states in the gap are controlled by the magnetic field. They might be donor and/or acceptor levels as in the case of impurity levels in a semiconductor. The discrete levels and their dependence on the magnetic flux along the tube axis are characterized by whether $l-m$ is a multiple of 3 or not. This rule about l and m reflects the band structure of the nanotube without the cap[8,9] and suggests that the n-(1,0) cap and the n-(1,1) cap whose localized states can be analytically given have some common features with general n-(l,m) caps. When $l=m$, the symmetric localized state appears only in the band $\beta=0$ and it becomes a resonant state for a finite value of β, while the other localized states appear for a finite range of β.

ACKNOWLEDGMENTS

We would like to thank Dr. Katsuyoshi Kobayashi for useful suggestions about the critical state. This work is supported in part by a Grant-in Aid for Scientific Research from the Ministry of Education, Science and Culture.

[1]H. W. Kroto, J. R. Heath, S. C. O'Brien, R. F. Curl, and R. E. Smalley, Nature (London) **318**, 162 (1985); W. Krätschmer, L. D. Lamb, K. Fostiropoulos, and D. R. Huffman, *ibid.* **347**, 354 (1990); G. Meijer and D. S. Bethune, Chem. Phys. **175**, 1 (1990).

[2]S. Iijima, Nature (London) **354**, 56 (1991); S. Iijima, T. Ichihashi, and Y. Ando, *ibid.* **356**, 776 (1992).

[3]S. Amelinckx *et al.*, Science **265**, 635 (1994); X. B. Zhang *et al.*, Europhys. Lett. **27**, 141 (1994); V. Ivanov *et al.*, Chem. Phys. Lett. **223**, 329 (1994); C. H. Kiang *et al.*, J. Phys. Chem. **98**, 6612 (1994).

[4]S. Ihara, S. Itoh, and J. Kitakami, Phys. Rev. B **48**, 5643 (1993); K. Akagi, R. Tamura, M. Tsukada, S. Itoh, and S. Ihara, Phys. Rev. Lett. **74**, 2307 (1995).

[5]D. Ugarte, Nature (London) **359**, 707 (1992).

[6]S. Itoh, S. Ihara, and J. Kitakami, Phys. Rev. B **47**, 1703 (1993); S. Ihara, S. Itoh, and J. Kitakami, *ibid.* **47**, 12 908 (1993); S. Itoh and S. Ihara, *ibid.* **48**, 8323 (1993); B. I. Dunlop, *ibid.* **46**, 1933 (1992).

[7]D. Vanderbilt and J. Tersoff, Phys. Rev. Lett. **68**, 511 (1992); A. L. Mackay and H. Terrones, Nature (London) **352**, 762 (1991); T. Lenosky, X. Gronze, M. Teter, and V. Elser, *ibid.* **355**, 333 (1992); N. Hamada, in *Physics and Chemistry of Nanometer-Scale Materials,* Proceedings of the 4th NEC Symposium of Fundamental Approaches to New Material Phases, edited by Y. Nishina, M. Mizuta, and H. Kamimura (Elsevier Sequoia, Japan, 1993), pp. 181.

[8]M. S. Dresselhaus, G. Dresselhaus, and R. Saito, Solid State Commun. **84**, 201 (1992).

[9]R. Saito, M. Fujita, G. Dresselhaus, and M. S. Dresselhaus, Phys. Rev. B **46**, 1804 (1992); J. W. Mintmire, B. I. Dunlop, and C. T. White, Phys. Rev. Lett. **68**, 631 (1992); N. Hamada, S. Sawada, and A. Oshiyama, *ibid.* **68**, 1579 (1992).

[10]R. Tamura and M. Tsukada, Phys. Rev. B **49**, 7697 (1994).

[11]M. Fujita, R. Saito, M. S. Dresselhaus, and G. Dresselhaus, Phys. Rev. B **45**, 13 834 (1992).

[12]R. Haydock, V. Heine, and M. J. Kelly, J. Phys. C **5**, 2845 (1972).

[13]C. A. Coulson and R. Taylor, Proc. R. Soc. London A **65**, 815 (1952).

[14]H. Ajiki and T. Ando, J. Phys. Soc. Jpn. **62**, 1255 (1993).